PROCEEDINGS OF SCIENCE

Higgs properties

Johannes Brandstetter[*†]
Institute of High Energy Physics (HEPHY) Vienna
E-mail: johannes.brandstetter@cern.ch

ATLAS and CMS analyses of the most important decay channels are outlined and measurements of Higgs boson properties are summarized and compared with standard model expectations. This report presents ATLAS and CMS analyses with LHC run 1 data taken at centre-of-mass energies of $\sqrt{s} = 7$ TeV and $\sqrt{s} = 8$ TeV as well as the latest analyses with 2015 LHC run 2 data taken at a centre-of-mass energy of $\sqrt{s} = 13$ TeV.

Flavor Physics and CP Violation,
6-9 June 2016
Caltech, Pasadena CA, USA

[*]Speaker.
[†]On behalf of the ATLAS and the CMS Collaboration.

PoS(FPCP2016)025

1. Introduction

In 2012 the discovery of a new boson with a mass of about 125 GeV was announced by ATLAS and CMS [1, 2]. Later on the new boson was established as standard model (SM) like Higgs boson, predicted nearly 50 years ago, since its properties agree very well with SM expectations. ATLAS and CMS [3, 4] collected data at a centre-of-mass energy of $\sqrt{s} = 7$ TeV in 2011, $\sqrt{s} = 8$ TeV in 2012 and $\sqrt{s} = 13$ TeV in 2015, corresponding to integrated luminosities of approximately 5 fb^{-1}, 20 fb^{-1} and 3 fb^{-1} respectively. The main goal of this article is to summarize Higgs boson measurements and consider their compatibility with SM predictions. Firstly, the five most sensitive decay channels, namely H $\rightarrow$ ZZ $\rightarrow$ 4l, H $\rightarrow \gamma\gamma$, H $\rightarrow$ WW, H $\rightarrow \tau\tau$ and H $\rightarrow$ bb are compared. Furthermore, a special focus is on the properties of the Higgs boson, especially on combined ATLAS and CMS results. LHC run 1 results are complemented with first LHC run 2 results, wherever results are already available. Some small excess of events are discussed which are directly related to the Higgs boson properties.
During LHC run 1 roughly 1 million Higgs bosons were produced. The production happens mainly in 4 distinct production modes: Gluon-gluon fusion (ggF), vector-boson fusion (VBF), associated W/Z production (WH/ZH) and production with associated top/bottom quark pairs (ttH, bbH). Table 1 summarizes the production modes for different centre-of mass energies. The rates of all production modes increase with increasing centre-of-mass energies, e.g. ttH production increases by a factor of 4 for a centre-of-mass energy increase of $\sqrt{s} = 8$ TeV to $\sqrt{s} = 13$ TeV.

	SM Higgs boson cross section [pb]		
mode	7 TeV	8 TeV	13 TeV
ggH	15.31	19.47	44.14
VBF	1.24	1.60	3.78
WH	0.58	0.70	1.37
ZH	0.34	0.42	0.88
ttH	0.09	0.13	0.51
bbH	0.16	0.20	0.49

Table 1: Production modes of a SM 125 GeV Higgs boson at different LHC centre-of-mass energies [5] and centred values of predictions for their cross sections

2. The most sensitive five decay channels

2.1 H $\rightarrow$ ZZ $\rightarrow$ 4l

The H $\rightarrow$ ZZ branching ratio is of about 2.6% at a Higgs boson mass of 125 GeV. Since the signature is very clean in the four lepton final state, H $\rightarrow$ ZZ $\rightarrow$ 4l has a high search sensitivity at the LHC. The final states consist of pairs of muons and electrons: 4μ, 4e or 2μ2e. The four-lepton mass is measured over a small continuum background. The most dominant irreducible background arises from directly produced nonresonant ZZ and Zγ^* events. Due to the clear signature the H $\rightarrow$ ZZ $\rightarrow$ 4l channel is well-suited for Higgs boson mass measurements. The LHC run 1 final m_{4l}

plots are shown in Fig. 1 [6, 7]. LHC run 2 results at a centre-of-mass energy of $\sqrt{s} = 13$ TeV can be found in Ref. [8, 9]. Both ATLAS and CMS measured cross sections of the Higgs boson as a function of the centre-of mass energy (7 TeV, 8 TeV, 13 TeV). ATLAS results for combined inclusive cross section measurements of the H $\rightarrow$ ZZ and the H $\rightarrow \gamma\gamma$ channel can be found in Ref. [10]. CMS results for H $\rightarrow$ ZZ $\rightarrow$ 4l fiducial cross sections can be found in Ref. [9].

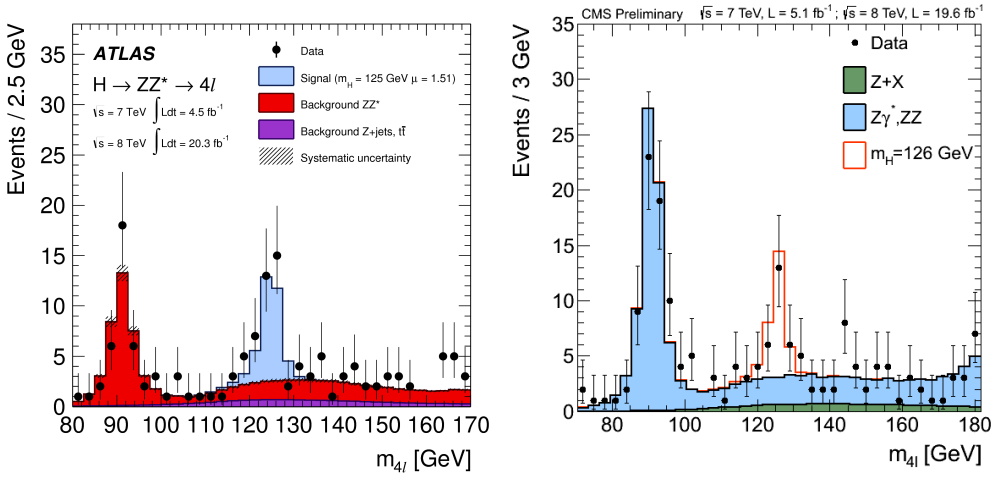

Figure 1: LHC run 1 results for H $\rightarrow$ ZZ $\rightarrow$ 4l of ATLAS (left) and CMS (right) [6, 7].

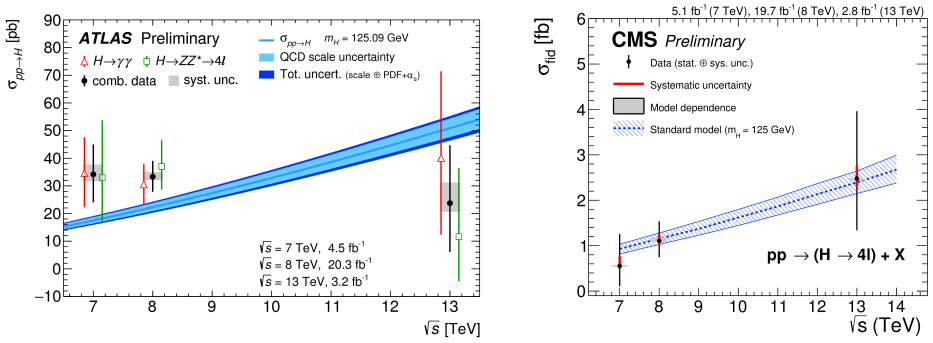

Figure 2: ATLAS inclusive cross section measurements combining H $\rightarrow \gamma\gamma$ and H $\rightarrow$ ZZ $\rightarrow$ 4l final states (left), CMS fiducial cross section measurements for the Higgs boson at different centre-of mass energies (left) [9, 10].

2.2 H $\rightarrow \gamma\gamma$

ATLAS and CMS results for the 2015 dataset can be found in [13][14]. The H $\rightarrow \gamma\gamma$ branching ratio is relatively small ($< 0.23\%$). The selected events are split into different categories depending on the signal purity and the mass resolution. The estimation of the underlying diphoton background is performed by a fit to the observed diphoton mass distribution. Similar to the H $\rightarrow$ ZZ $\rightarrow$ 4l

channel the H $\rightarrow \gamma\gamma$ is well suited for mass measurements of the Higgs boson due to precise energy reconstruction of the photons in the electromagnetic calorimeter. The LHC run 1 final $m_{\gamma\gamma}$ plots are shown in Fig. 3 [11, 12], LHC run 2 results at a centre-of-mass energy of $\sqrt{s} = 13$ TeV can be found in Ref. [13, 14].

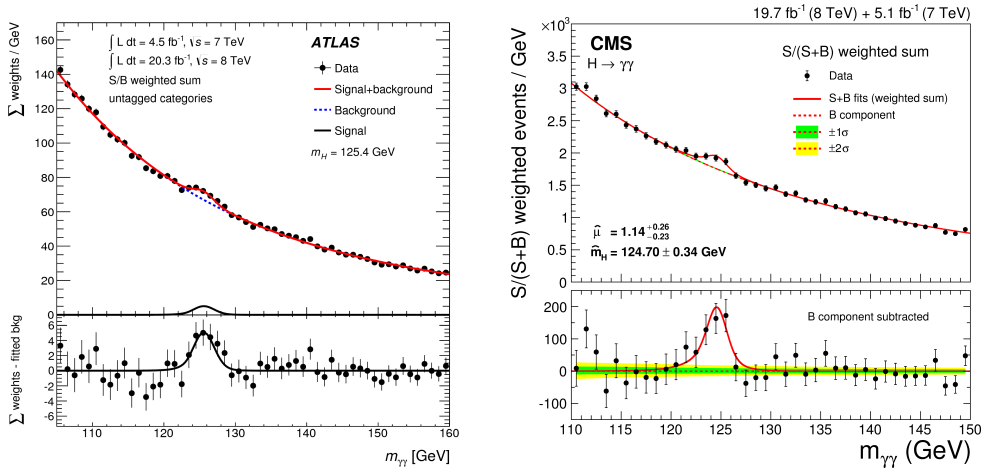

Figure 3: LHC run 1 diphoton invariant mass distribution of ATLAS (right) and CMS (left), the lower parts of the plots display the mass distribution after background subtraction [13, 14].

2.3 H $\rightarrow$ WW $\rightarrow$ 2l2ν, H $\rightarrow \tau\tau$, H $\rightarrow$ bb

H $\rightarrow$ WW has a branching ratio of about 22% which is the second highest. The event signatures of H $\rightarrow$ WW $\rightarrow$ 2l2ν are amongst others either two opposite-signed leptons in the final states which targets ggF and VBF production modes, or for VH production three leptons with a combined charge of ± 1. Due to neutrinos in the final state no full mass reconstruction is possible. The measured significances are 6.1σ (5.8σ exp.) at ATLAS and 4.3σ (5.8σ exp.) at CMS [15, 20].
Whereas H $\rightarrow$ ZZ $\rightarrow$ 4l, H $\rightarrow \gamma\gamma$ and H $\rightarrow$ WW $\rightarrow$ 2l2ν all are bosonic decay modes, the best fermionic decay candidate and thus the best candidate to directly probe a Yukawa coupling is H $\rightarrow \tau\tau$ which has a branching ratio of about 6%. Since the τ lepton can decay both hadronically and leptonically into electrons or muons the H $\rightarrow \tau\tau$ analysis deals with several final states. Due to neutrinos missing transverse energy occurs in every final state. While the individual LHC run 1 analyses are still below 5σ [16, 21] the combination of ATLAS and CMS results already exceeds 5σ [17, 18].
With about 58% H $\rightarrow$ bb has the highest branching ratio. The overwhelming QCD background limits the analyses since e.g. ggF production modes can not be exploited. The searches are performed in VBF production mode as well as associated VH and associated ttH production. Run 1 results show significances of 1.4σ (2.6σ exp.) from ATLAS and 2.1σ (2.1σ exp.) from CMS, respectively [19, 22].

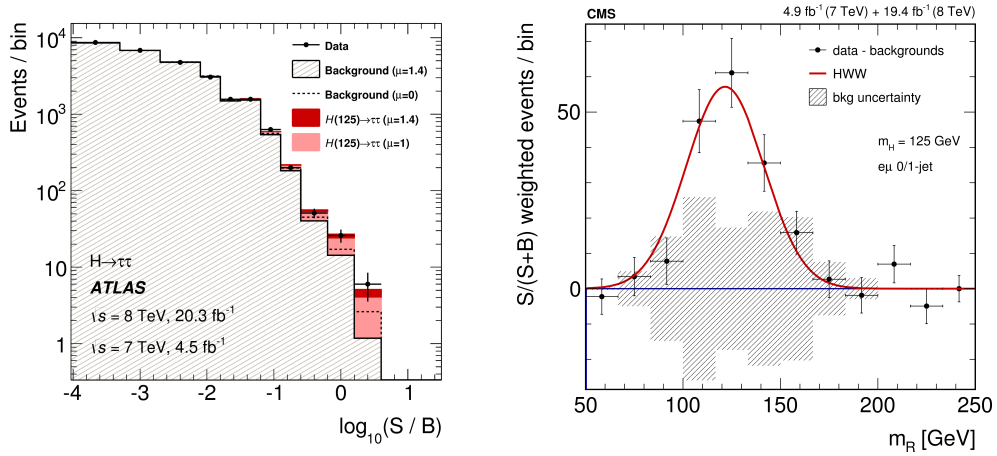

Figure 4: Event yields as a function of $x\log(\mathrm{S}/\mathrm{B})$ in the $\mathrm{H} \to \tau\tau$ channel from ATLAS (left), LHC run 1 results in the $\mathrm{H} \to \mathrm{WW} \to 2\mathrm{l}2\nu$ from CMS (right) [16, 20].

3. Higgs boson properties

For most of the following Higgs boson property measurements the five decay channels mentioned above or a subset of them are used.

3.1 Mass and total width

The precise measurement of the Higgs boson mass is particularly important since a well known mass allows to predict all properties of a SM Higgs boson. An ATLAS and CMS combination of LHC run 1 results on the Higgs boson mass can be found in Ref. [23]. Taking both channels $\mathrm{H} \to \mathrm{ZZ} \to 4\mathrm{l}$ and $\mathrm{H} \to \gamma\gamma$ into account and combining both experiments yields a Higgs boson mass of $m_H = 125.09 \pm 0.21(\mathrm{stat.}) \pm 0.11(\mathrm{syst.})$ GeV which has uncertainties already at the per mille-level. The result is compatible with both SM as well as MSSM. In order to obtain the results a simultaneous fit is applied to the $\mathrm{H} \to \mathrm{ZZ} \to 4\mathrm{l}$ and the $\mathrm{H} \to \gamma\gamma$ mass peaks. The resulting masses are found to be consistent with each other. The results are depicted in Fig. 5.
The total width of the Higgs boson is expected to be small ($\Gamma_{\mathrm{H}}^{\mathrm{SM}} \sim 4$ MeV), in contrast to Γ_{Z} and $\Gamma_{\pm\mathrm{W}}$ ($\Gamma \sim O(\mathrm{GeV})$). Results can be found in Ref. [24, 25].
In order to measure the total width (Γ) of the Higgs boson $\mathrm{H} \to \mathrm{ZZ} \to 4\mathrm{l}$ events are used. Direct measurements allow to constrain $\Lambda_{\mathrm{H}} < O(\mathrm{GeV})$. A different approach is to study off-shell and on-shell Higgs boson production cross sections

$$\left.\begin{aligned} \sigma^{\mathrm{on}}_{i\to H\to f} &\propto \frac{g_i^2 g_f^2}{\Gamma_{\mathrm{H}}} \\ \sigma^{\mathrm{off}}_{i\to H\to f} &\propto g_i^2 g_f^2 \end{aligned}\right\} \frac{\sigma_{\mathrm{off}}}{\sigma_{\mathrm{on}}} = \Gamma_{\mathrm{H}}, \tag{3.1}$$

where g_i is the coupling to the initial and g_f the coupling to the final state. This measurement, however, makes several assumptions and is thus model-dependent.

Off-shell contributions mostly arise due to the proximity of the ZZ threshold. The analyses allow to constrain $\Gamma_H/\,\Gamma_{SM} < 5-8\ (7-12)$ obs. (exp.) at ATLAS and $\Gamma_H/\,\Gamma_{SM} < 5.4\ (8.0)$ obs. (exp.) at CMS, respectively.

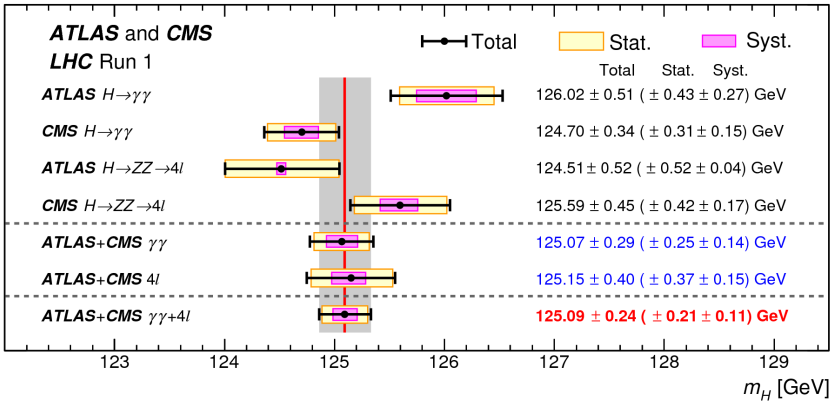

Figure 5: LHC run 1 combination of ATLAS and CMS results on the Higgs boson mass [23].

3.2 Signal strength

The signal strength amplifier μ is defined as

$$\mu = \frac{\mu_{if}^{obs}}{\mu_{if}^{SM}} = \frac{\sigma_i^{obs}}{\sigma_i^{SM}} \cdot \frac{BR_f^{obs}}{BR_f^{SM}}\,, \tag{3.2}$$

where $\sigma_i^{obs(SM)}$ is the observed (by the SM predicted) production cross section and BRobs(SM) the observed (by the SM predicted) branching ratio. Since the signal strength amplifier μ is a product of production cross sections and branching ratios assumptions have to be made. SM production modes are assumed for measuring the μ values of the individual branching ratios and SM branching ratios are assumed for measuring the μ values of the individual production modes. Individually tagged production and decay measurements show good agreement with SM predictions. The combined ATLAS and CMS result adds up to $\mu = 1.09 \pm 0.11$ which is also in good agreement with the SM expectation. The ratio of bosonic (μ_{VBF}, μ_{VH}) and fermionic (μ_{ggF}, μ_{ttH}) production modes provides an important consistency check of the SM. The combined ATLAS and CMS result on the ratio of bosonic and fermionic production modes is $1.06^{+0.35}_{-0.27}$. ATLAS and CMS results on the signal strength amplifier μ can be found in [26, 27]. Fig. 6 depicts summary plots of the μ values of the individually tagged production modes and branching rations.
A modest 2σ excess of events shows up in the ttH tagged production mode which is mostly driven by the CMS same-sign dilepton channel where leptons come from a W boson, a Z boson, a tau lepton or a top quark. So far no significant discrepancy has been seen in other measurements where Higgs-top couplings are involved, e.g. ggF tagged events or $H \to \gamma\gamma$ events. The individual analyses can be found in [28, 29]. Since the ttH production mode increases by a factor of about 4 for a centre-of-mass energy increase from $\sqrt{s} = 8$ TeV to $\sqrt{s} = 13$ TeV the 2015 dataset corresponds

already to half of the run 1 dataset. CMS combination of $\gamma\gamma$, multilepton and bb final state yields a value of $\mu_{\mathrm{ttH}} = 0.15^{+0.95}_{-0.85}$ [30, 31, 32]. Another small discrepancy can be seen in the likelihood scan over $\mathrm{BR}^{\mathrm{bb}}/\mathrm{BR}^{\mathrm{ZZ}}$. The overall deficit is 2.5σ.

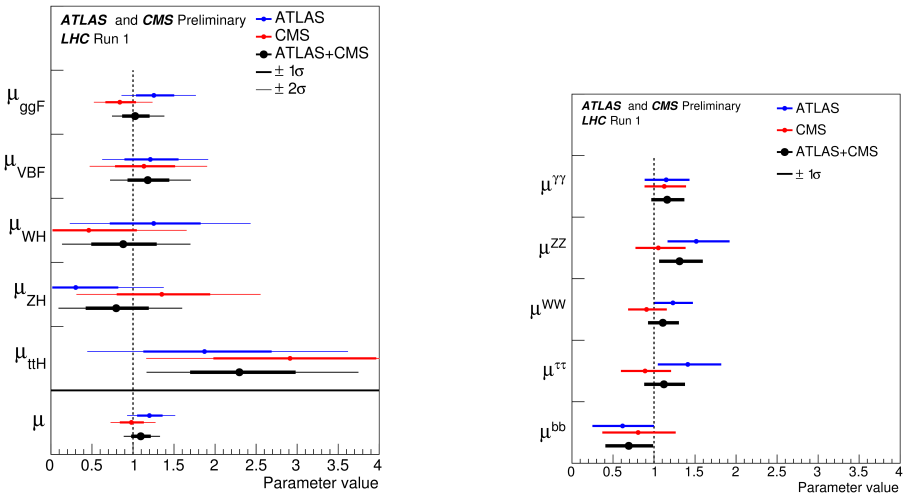

Figure 6: Combined ATLAS and CMS μ values of the individually tagged production modes (left) and branching ratios (right) [26, 27].

3.3 Couplings

The event yield for a production mode i and a final state f assuming narrow width approximation reads

$$(\sigma \cdot \mathrm{BR})\,(i \to \mathrm{H} \to f) = \frac{\sigma_i \cdot \Gamma_f}{\Gamma_{\mathrm{tot}}}, \tag{3.3}$$

where BR is the branching ratio, Γ_f the partial decay width into the final state and Γ_{tot} the total width of the Higgs boson. The coupling strength modifiers κ_i are introduced with respect to the SM values as

$$\kappa_i^2 = \frac{\Gamma_{ff}}{\Gamma_{ff}^{\mathrm{SM}}} = \frac{\sigma_i}{\sigma_i^{\mathrm{SM}}}, \tag{3.4}$$

where Γ_{ff} is the total decay width into the final state ff and σ_i the production cross section. Similar to measurements of the signal strength modifiers also for the coupling strength modifiers assumptions have to be made, e.g. that there are no beyond the SM contributions or that the couplings to vector bosons do not exceed the SM expectation value of 1. The effect on the results can be seen in the left plot in Fig. 7. Since the coupling of the Higgs boson to vector bosons and fermions are based on two different mechanisms, electroweak symmetry breaking and Yukawa coupling, a 2D likelihood scan over the (κ_f, κ_V) parameter space is performed to provide an important SM consistency check. Any significant deviation from $(\kappa_f, \kappa_V) = (1, 1)$ would clearly indicate a discrepancy with respect to the SM. The combined ATLAS and CMS value of all five decay channels shows good agreement with the SM expectation, as shown in the right plot of Fig. 7 [26, 27].

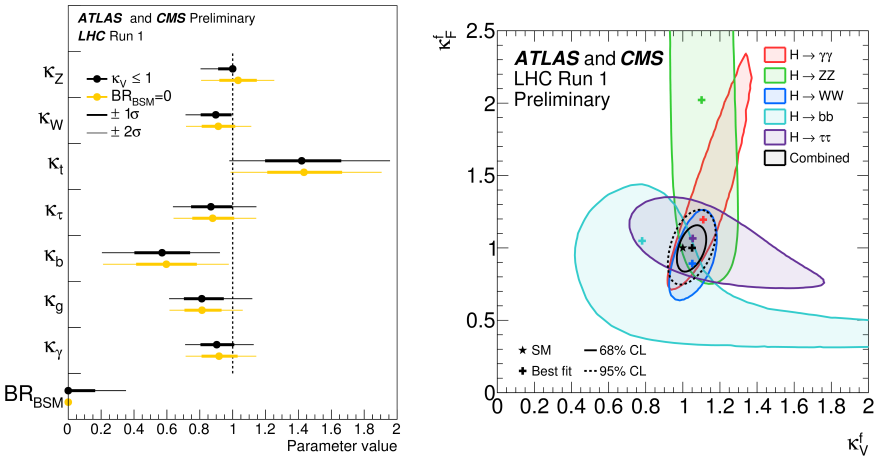

Figure 7: Results on coupling strength modifiers measurements using different assumptions (left), results on the 2D likelihood scan over the (κ_f, κ_V) parameter space (right) [26, 27].

3.4 Spin and parity

ATLAS and CMS results on spin and parity measurements of the Higgs boson can be found in [33, 34]. The SM predicts a Higgs boson with zero spin and positive parity (0^+). For Spin-parity studies $H \to ZZ \to 4l$, $H \to \gamma\gamma$ and $H \to WW \to l\nu l\nu$ events are taken. A test statistic

$$q = -2 \cdot \ln\left(\frac{L_{J^P}}{L_{0^+}}\right) \tag{3.5}$$

is dfined for different J^P models and tested against the 0^+ SM Higgs boson hypothesis. A wide range of various alternative J^P hypotheses is excluded at 99% confidence level or higher. Any mixed-parity spin-one state is excluded in the ZZ and WW modes at a confidence level greater than 99.999%. The results are consistent with a SM Higgs boson with zero spin and positive parity. Nevertheless, still chances of mixtures of anomalous 0^+ and 0^- contributions exist. Figure 8 shows the results on various J^P hypotheses.

4. Summary and outlook

During LHC run 1 the Higgs boson was discovered by both ATLAS and CMS. Some production modes as well as individual decay channels are already measured with a significance $> 5\sigma$. So far the Higgs boson looks very SM like with a good agreement of ATLAS and CMS results and also with SM predictions. The mass of the Higgs boson is measured in the $H \to ZZ \to 4l$ and $H \to \gamma\gamma$ channel to be $m_H = 125.09 \pm 0.21(\text{stat.}) \pm 0.11(\text{syst.})$ GeV with uncertainties in the per mille-level. Studies of off-shell and on-shell Higgs boson production allow to constrain $\Gamma_H/\ \Gamma_{SM} < 5-8\ (7-12)$ obs. (exp.) at ATLAS and $\Gamma_H/\ \Gamma_{SM} < 5.4\ (8.0)$ obs. (exp.) at CMS, respectively. This measurement, however, makes several assumptions and is thus model-dependent. Signal strength and coupling amplifier measurements also show good consistency with SM expectations and good agreement between bosonic and fermionic channels. Small SM tensions

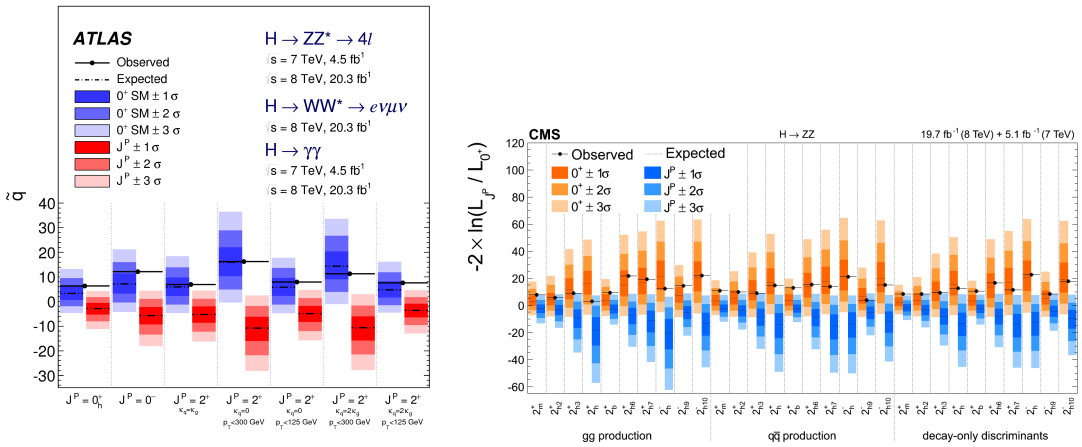

Figure 8: ATLAS results (left) and CMS results (right) on various J^P hypotheses [33, 34].

which are directly related to Higgs boson properties can be seen in the ttH production mode and in BR^{bb}/BR^{ZZ}. More data is needed to further investigate these deviations. Spin-parity measurements are consistent with the 0^+ SM hypothesis.
LHC run 2 is expected to deliver approximately 150 fb^{-1} until the end of 2018 and approximately 300 fb^{-1} until the end of 2023. The coupling measurements of the Higgs boson will start to enter a really interesting regime since the uncertainties will will go down to a few percent (compared to $20\% - 30\%$ today). After the long shutdown 3 the high-luminosity LHC run is planned to start and to deliver approximately 3000 fb^{-1} until 2037.

References

[1] ATLAS Collaboration, Phys. Lett. B 716, 1 (2012).

[2] CMS Collaboration, Phys. Lett. B 716, 30 (2012).

[3] ATLAS Collaboration, JINST 3 S08003 (2008).

[4] CMS Collaboration, JINST 3 S08004 (2008).

[5] LHC Higgs Cross Section Working Group, 'Handbook of LHC Higgs Cross Sections: 3. Higgs Properties', arXiv:1307.1347 (2013), and updates presented on 'https://twiki.cern.ch/twiki/bin/view/LHCPhysics/LHCHXSWG'.

[6] ATLAS Collaboration, Phys. Rev. D 91, 012006 (2015).

[7] CMS Collaboration, Phys. Rev. D 89, 092007 (2014).

[8] ATLAS Collaboration, ATLAS-CONF-2015-059.

[9] CMS Collaboration, CMS-PAS-HIG-15-004.

[10] ATLAS Collaboration, ATLAS-CONF-2015-069.

[11] ATLAS Collaboration, Phys. Rev. D 90, 112015 (2014).

[12] CMS Collaboration, EPJ C 74 3076 (2014).

[13] ATLAS Collaboration, ATLAS-CONF-2015-060.

[14] CMS Collaboration, CMS-PAS-HIG-15-006.

[15] ATLAS Collaboration, Phys. Rev. D 92, 012006 (2015).

[16] ATLAS Collaboration, JHEP04 117 (2015).

[17] ATLAS Collaboration, ATLAS-CONF-2015-044.

[18] CMS Collaboration, CMS-PAS-HIG-15-002.

[19] ATLAS Collaboration, ATLAS-CONF-2012-161.

[20] CMS Collaboration, JHEP01 096 (2014).

[21] CMS Collaboration, JHEP05 104 (2014).

[22] CMS Collaboration, Phys Rev D.89.012003 (2014).

[23] ATLAS and CMS Collaboration, PhysRevLett.114.191803 (2015).

[24] ATLAS Collaboration, ATLAS-CONF-2014-042.

[25] CMS Collaboration, PLB 736 64 (2014).

[26] ATLAS Collaboration, ATLAS-CONF-2015-044.

[27] CMS Collaboration, CMS-PAS-HIG-15-002.

[28] ATLAS Collaboration, HEP 09 (2014) 087.

[29] CMS Collaboration, Phys. Lett. B 749 (2015) 519-541.

[30] CMS Collaboration, CMS-PAS-HIG-15-005.

[31] CMS Collaboration, CMS-PAS-HIG-15-008.

[32] CMS Collaboration, CMS-PAS-HIG-16-004.

[33] ATLAS Collaboration, EPJ C 75, 476 (2015).

[34] CMS Collaboration, Phys. Rev. D 92, 012004 (2015).